

Durability of anodic aluminum oxide (AAO) films formed on technically pure AA1050 alloy against corrosion

Ch. A. Girginov*, S. V. Kozhukharov, M. J. Milanec

University of Chemical Technology and Metallurgy, 8 St. Kliment Ohridski Blvd., 1756 Sofia, Bulgaria

Received June 03, 2017; Accepted October 07, 2017

The present research provides data about the remarkable durability of Anodized Aluminum Oxide (AAO) film grown on technically pure AA1050 alloy during and after extended exposure to 3.5% NaCl model corrosive medium. The samples were cut from thick aluminum foil with approximate dimensions 30 x 30 mm. The anodization was performed for 48 min in 15% wt. H₂SO₄ in galvanostatic (15 mA cm⁻²) and isothermal (20 °C) regime. This process was carried out in a two electrode cell with continuous stirring. The obtained AAO films were submitted to regular weekly electrochemical measurements via Electrochemical Impedance Spectroscopy (EIS) and Linear Sweep Voltammetry (LSV). The EIS spectra have shown almost pure capacitive behavior of the investigated samples. This fact is an indication for the well-expressed insulating capability of the obtained AAO films. Furthermore, the specimens kept their capacitance during the entire exposure period, showing remarkable AAO durability. Only gradual EIS spectra shape evolution was registered, without any abrupt changes. The obtained spectra were further submitted to quantitative data fitting analysis to suitable equivalent circuits. The EIS results were further confirmed by the LSV measurements. The registered currents were in the range of the equipment minimum detection threshold, confirming the assumption for the purely capacitive AAO behavior. The obtained data reveal that the formed AAO films efficiently protect the metallic substrates even after 5208 hours of exposure without any indication for corrosion damage.

Keywords: Anodization, Alumina films, EIS, LSV

INTRODUCTION

Pure aluminum and its low doped alloys find various applications in both mass production and hi-tech industrial sectors. One of the widest fields of use of this metal is the packaging of various nutrition products and soft drinks [1-4]. However, reliable packaging requires additional surface protection of the Al-based packaging materials, prior to contact with whatever nutrition product. This requirement has arisen because Al-ions resorption was recently evinced from such packaging products [5-7], which can be dangerous for the human health [8, 9]. The specific conjunction of electrical conductivity with the strength to weight ratio [10-12] makes aluminum an indispensable material for high voltage, long distance electricity distribution [13-16]. Aluminum rolls with precisely textured AAO surfaces are widely used for ink-printing on paper and plastic packaging materials [17-20], and even for production of flexible solar cells by printing [21].

Anodization is a relatively simple process, which at defined conditions enables the formation of highly ordered oxide layers with various possible applications in the hi-tech industrial branch. The AAO films are representative for the so called "self-assembled monolayers" (SAM) [22]. Besides, both the porous and barrier AAO layers can be

successfully used for large series of Metal Oxide Semiconductor (MOS), Metal Dielectric Semiconductor (MDS) and Metal Oxide Semiconductor Field Effect (MOSFE) high performance transistors and integral micro-schemes, based on these electronic elements [23-25]. The capabilities of the anodized aluminum self-assembled layers have recently been investigated for fuel cell electrodes [26] and even for gas analysis sensors [27] and biosensors [28].

The aim of the present research work is to provide information regarding the durability of porous AAO layers on AA1050 substrates in a conventional 3.5% NaCl model corrosive medium. The experiments were performed by regular (once per week) electrochemical measurements via Electrochemical Impedance Spectroscopy (EIS) and Linear Sweep Voltammetry (LSV) for extended exposure times, up to 5208 hours.

EXPERIMENTAL

A set of samples of technically pure aluminum (AA1050) were submitted to anodization and subsequent electrochemical measurements. The samples were preliminary etched in 50 g dm⁻³ NaOH solution at 60°C and then activated in diluted (1:1 v/v) HNO₃ at room temperature. Both operations were performed for two minutes. The

* To whom all correspondence should be sent.
E-mail: christian.girginov@gmail.com

anodization was performed for 48 min. in 15% wt. H_2SO_4 in galvanostatic (15 mA cm^{-2}) and isothermal ($20 \text{ }^\circ\text{C}$) regime, after vigorous cleaning by tap and distilled water. This process was carried out in a two electrode cell (250 ml) with continuous stirring. The actual working zones, submitted to anodization were with a diameter of 24.5 mm for all samples.

The already anodized samples were then put through electrochemical characterizations, using Electrochemical Impedance Spectroscopy (EIS) and Linear Sweep Voltammetry (LSV) as measurement techniques. The respective measurements were carried out regularly (once per week), until 5208 hours of exposure to 3.5% NaCl (100 ml) model corrosive medium. The sample exposure was carried out in three electrode cells with Ag/AgCl/3M KCl reference electrode and a platinum cylindrical counter-electrode. Only part of the anodized zones (diam. 16 mm) was exposed to the electrolyte, in order to avoid any edge effects.

The EIS data acquisition was performed in the frequency range from 10^4 to 10^{-2} Hz, distributed in 50 steps at 120 mV, according to the Open Circuit Potential (OCP). This excitation signal amplitude was selected in order to overcome the high oxide layer resistance. After each EIS spectrum recording, individual LSV curves were recorded from +30 to -500 mV (in cathodic direction) and from -30 to +600 mV (in anodic direction),

respectively. The cathodic curves were acquired immediately after the EIS spectra acquisition, whereas the anodic ones were recorded after several hours of retention at OCP. This measurement cycle organization was selected for avoiding any polarization effects from the cathodic curves, on the shape of the anodic ones. The LSV curves in both directions were recorded with a potential sweep rate of 10 mV s^{-1} , in order to avoid any electrode damage due to excessive polarization.

RESULTS AND DISCUSSION

The visual inspection of the investigated samples (after 5208 hours of exposure to model corrosive medium) has shown lack of any notable features of localized corrosion attack whatsoever.

Since all specimens revealed absence of any corrosion activity, the possible AAO deterioration caused by the corrosive medium was evaluated by precise data analysis of the performed electrochemical measurements.

Electrochemical impedance spectroscopy *Initial EIS spectra acquisition*

The EIS spectra, acquired after 168 hours of exposure resemble capacitors, due to the well-defined barrier properties of the formed AAO layers. An example for the EIS spectra of three samples is shown in Fig. 1.

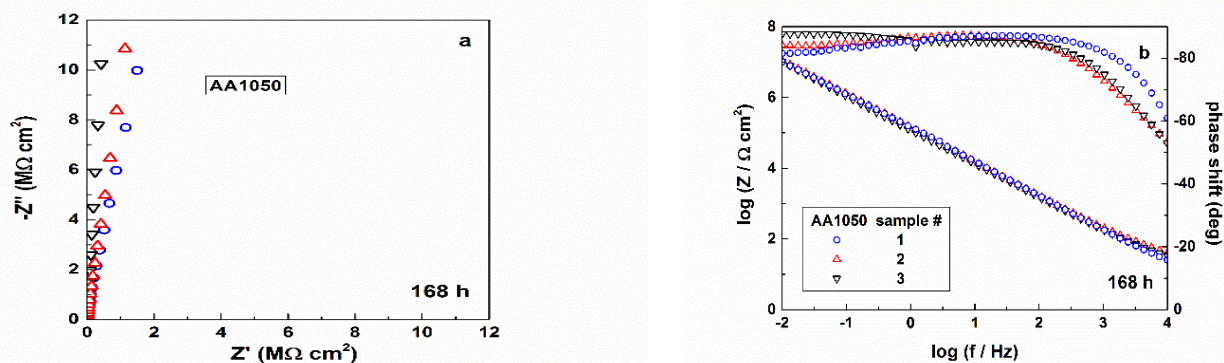


Fig.1. EIS spectra of three samples, recorded after 168 hours of exposure: Nyquist (a) and Bode (b) plots.

Besides, obviously the spectra in Fig. 1 almost completely overlap, indicating the remarkable reproducibility of the obtained AAO films. In order to determine the AAO durability, the experiments have been extended for larger exposure times, up to 5208 hours. The obtained results are shown below.

EIS spectra shape evolution within the exposure to the model corrosive medium

Fig. 2 illustrates the typical EIS evolution trends during the sample exposure to the corrosive medium. The Nyquist plots (Fig. 2a) acquired after

336 hours, until 5208 hours of exposure, remain unchanged, being almost straight vertical lines. Since such lines are typical for electronic capacitors, it can be inferred that the AAO films grown on AA1050 substrates possess definitely insulating properties which do not suffer significant changes during the entire period of exposure.

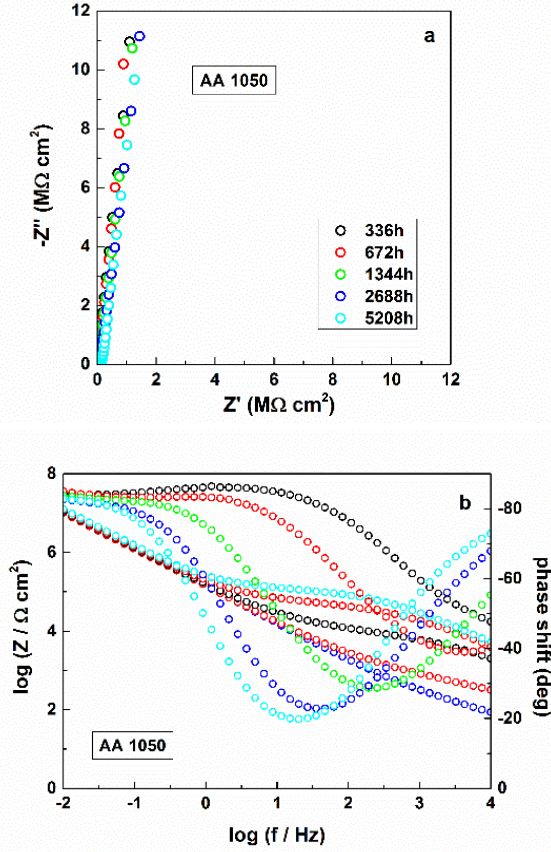
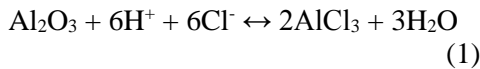
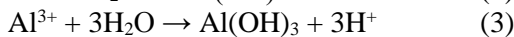
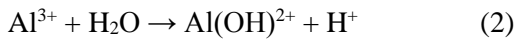


Fig. 2. Nyquist (a) and Bode (b) plots of typical EIS spectra, acquired after different exposure durations

The Bode plots (Fig. 2b) recorded after the same periods of time look more distinguishable from each other. The maxima of the $\phi/\log(f)$ lines displace towards the lower frequency range and at the high frequency range minima appear. Simultaneously, additional inflexions of the $\log|Z|/\log(f)$ curves appear, revealing an increase of the electrical resistance. This gradual change of the EIS spectra during the exposure, reveal coincident increase of the capacitive and the resistive components of the spectra. Both these trends reveal an AAO thickness decrease, combined with obstruction of the AAO pores and possible defects by insoluble corrosion products. These effects are probably result of the following reactions proceeding during the exposure of the AAO coated AA1050 samples to the model corrosive medium [29]:



Although the corrosive medium provides a neutral environment ($\text{pH} \approx 7$), local acidification appears near the metallic surface, according to [30]:



Alternatively, because the model corrosive medium was left to natural aeration, it contains dissolved oxygen and it can cause localized alkalization, following the reactions [30]:



The hydroxide anion generation causes additional attack against the AAO layer:



Both proposed chemical mechanisms result in AAO thickness decrease, combined by obstruction of the AAO pores and possible defects by insoluble corrosion products. The occurrence of such insoluble products with Keggin type cluster structures was proposed in previous works [31, 32]. This concept has served as a basis for the equivalent circuit description, commented below.

EIS modeling and quantitative data analysis

In order to obtain quantitative data, the acquired EIS spectra were fitted to suitable equivalent circuits, following the basic circuit description code (CDC) rules, proposed by Boukamp [33]. There, the capacitance elements are being used for description of charge transfer across interfaces, whereas the ohmic elements describe the charge transport through homogeneous medium. The spectra acquired after 168 hours of exposure were appropriate for fitting to an equivalent circuit, composed by two parallel RC-units, connected in series. However, after 336 hours of exposure, an additional constant phase element (CPE_{diff}) was necessary for data fitting. The need for this supplemental element is a consequence of the already occurred notable obstruction of the AAO pores by corrosion products, commented above. Consequently, the equivalent circuit suitable for EIS data fitting after 336 hours of exposure was composed by two time constants (i.e. parallel RC-units), with additional CPE, as illustrated in Fig. 3. The first element of the equivalent circuit is the model corrosive medium (electrolyte) resistance (R_{el}), which is consecutively connected with the first time constant ($C_{\text{oxy}}, R_{\text{oxy}}$). It is composed by the capacitance of the interface between the model corrosive medium and AAO (C_{oxy}) and the resistance of the electrolyte, within the pores of the oxide layer (R_{oxy}). The second time constant ($C_{\text{edl}}, R_{\text{ct}}$) can be ascribed to the interface between AAO and the metallic substrate. It comprises the electric double layer capacitance (C_{edl}) and the charge transfer resistance (R_{ct}). Finally, the additional constant phase element (CPE_{diff}) describes the

diffusion limitations caused by the corrosion product obstruction.

The quantitative data acquired by the fitting of the spectra shown in Fig. 2, to the equivalent circuits, illustrated in Fig.3 are summarized in Table 1 (for three of the investigated samples). It shows only the numerical values determined at 336 and 5208 hours of exposure, since it would be onerous to represent the obtained data from all recorded spectra (all exposure times).

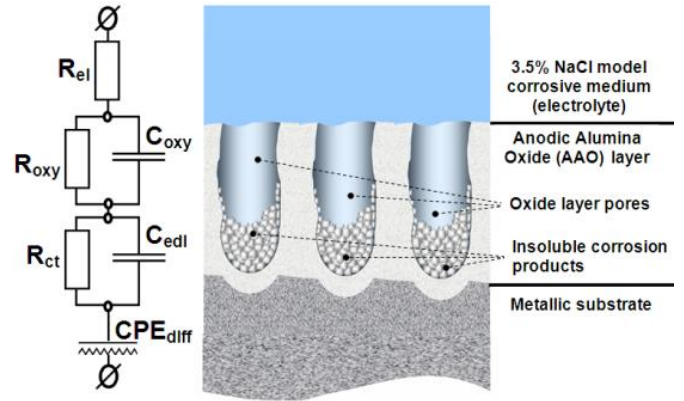


Fig. 3. Illustration of the equivalent circuit, suitable for EIS data fitting for extended exposure durations and the respective conceptual model.

Table 1. EIS data fitting results for the corrosion process kinetics

336 hours of exposure					
Element	Unit		Sample 1	Sample 2	Sample 3
R_{el}	$\Omega \text{ cm}^2$		29.94 ± 2.03	95.40 ± 6.12	30.7 ± 6.32
C_{oxy}	F cm^{-2}	10^{-7}	2.67 ± 0.21	2.97 ± 0.03	3.19 ± 0.26
R_{oxy}	$\Omega \text{ cm}^2$	10^3	0.49 ± 0.04	0.204 ± 0.002	0.48 ± 0.01
C_{edl}	F cm^{-2}	10^{-7}	1.16 ± 0.01	1.36 ± 0.06	1.44 ± 0.01
R_{ct}	$\Omega \text{ cm}^2$	10^3	0.17 ± 0.03	0.46 ± 0.02	0.24 ± 0.01
Q_{diff}	$\text{s}^n \Omega^{-1} \text{ cm}^{-2}$	10^{-7}	5.91 ± 0.31	6.36 ± 0.05	6.04 ± 0.89
n	-----		0.71 ± 0.02	0.82 ± 0.03	0.84 ± 0.02
5208 hours of exposure					
Element	Unit		Sample 1	Sample 2	Sample 3
R_{el}	$\Omega \text{ cm}^2$	10^3	2.44 ± 0.43	3.00 ± 0.63	2.80 ± 0.56
C_{oxy}	F cm^{-2}	10^{-9}	12.55 ± 2.88	11.78 ± 1.62	13.16 ± 1.69
R_{oxy}	$\Omega \text{ cm}^2$	10^3	163.40 ± 3.58	122.80 ± 8.65	131.40 ± 7.00
C_{edl}	F cm^{-2}	10^{-9}	3.34 ± 0.16	2.34 ± 0.10	2.58 ± 0.12
R_{ct}	$\Omega \text{ cm}^2$	10^3	63.60 ± 2.47	73.60 ± 7.21	60.80 ± 5.33
Q_{diff}	$\text{s}^n \Omega^{-1} \text{ cm}^{-2}$	10^{-7}	5.06 ± 0.10	4.88 ± 0.11	5.46 ± 0.12
n	-----		0.90 ± 0.01	0.88 ± 0.01	0.89 ± 0.01

The comparison of the data, represented in Table 1 shows that both C_{oxy} and C_{edl} , decrease by three orders of magnitude from 10^{-6} to $10^{-9} \text{ F cm}^{-2}$. The diffusion related constant phase element (CPE_{diff}), follows the same trend. However its coefficient (n) retains its value (around 1). This fact indicates that the CPE_{diff} resembles pure capacitance, resulting from the obstruction effect, caused by the insoluble corrosion products. Simultaneously, all the resistance elements: R_{el} , R_{oxy} and R_{ct} , increase in value, due to corrosion products accumulation. Consequently, the accumulation of polynuclear Keggin type $\text{Al}_x(\text{OH})_{3x-z}\text{Cl}_z$ corrosion products suppresses the Al-oxide layer thinning, by hindering the access of corrosive species to the surface.

The impedance spectra components do not follow similar trends of evolution (Fig. 4).

The R_{el} , initially increases progressively, and afterwards remains unchanged at about $3 \text{ k}\Omega \text{ cm}^2$. The rest resistance components R_{oxy} and R_{edl} tend to increase linearly. This difference of the resistance evolution kinetics can be explained, having in mind that R_{el} corresponds to the total accumulation of corrosion products on the entire sample surface, whereas R_{oxy} and R_{edl} are rather related only to the corrosion product accumulation inside the AAO pores and defects.

The capacitance elements show similar trends. Initially, C_{oxy} shows a sharp decrease, followed by reaching of almost steady state at about 2 nF cm^{-2} . The C_{edl} and CPE_{diff} suffer weak linear decrease with insignificant slope.

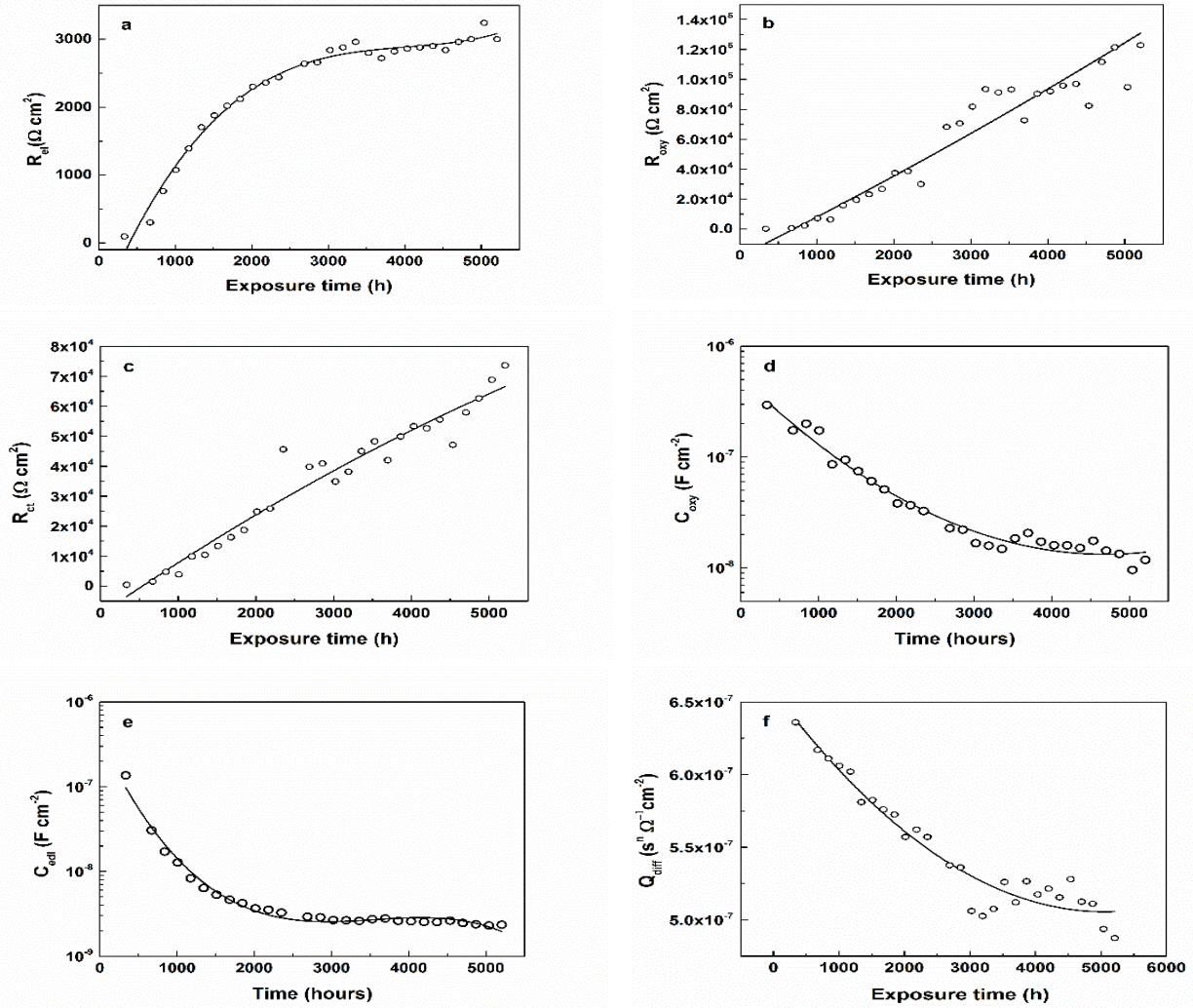


Fig. 4. Resistance (a - c), capacitance and CPE (d - f) values evolution during the exposure to the model corrosive medium

Linear sweep voltammetry

This method was used, because any eventual AAO breakdowns could easily be determined by the sharp changes of the respective LSV curves. Besides, this method enables the detection of localized corrosion activities [34], by the occurrence of sharp inflexions in the anodic LSV branches.

In the present case the LSV curves acquired even after 5208 hours of exposure to the model corrosive medium, remain at the equipment minimal current detection threshold (Fig. 5).

This fact obviously evinces the lack of any oxide film breakdowns for the entire period of

exposure (5208 hours), confirming the inferences done for the EIS measurements. The LSV curves are horizontal, revealing the passivation role of the AAO formed during anodization.

Summarizing the data obtained by both electrochemical methods, it can be concluded that the corrosion process of anodized AA1050 alloy in stationary hydrodynamic conditions is a self-inhibiting process, due to the insoluble corrosion products accumulation and the consequent pore obstruction. These processes suppress the corrosion process, because of the corrosive species hindering the inside of AAO pores and defects.

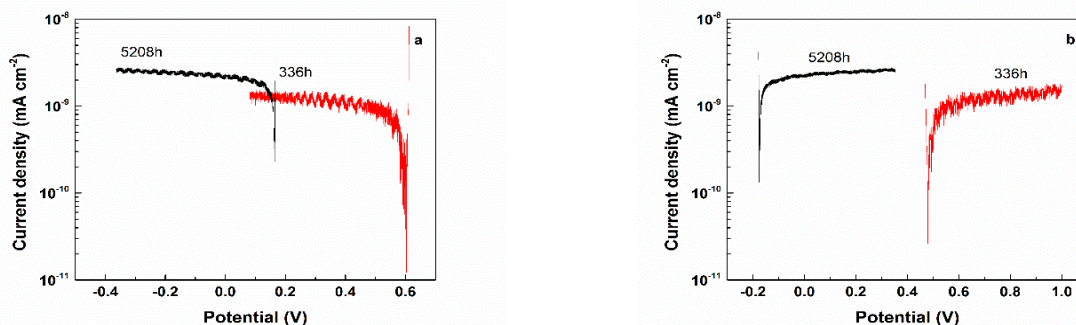


Fig. 5. Cathodic (a) and anodic (b) LSV curves, recorded for two exposure durations (336 and 5208 h)

CONCLUSIONS

The remarkable durability of Anodized Aluminum Oxide (AAO) layer grown on technically pure aluminum substrates in conventional 3.5% NaCl model corrosive medium was evaluated. The specimens did not show any remarkable indications for corrosion even after 5208 hours of exposure.

The acquired EIS spectra have shown almost pure capacitance, revealing the well-defined insulation properties of the obtained AAOs. Indeed, the phase shift approached 90 degrees. Besides, the spectra shapes changed gradually, due to lack of any film breakdowns for the entire exposure period.

A quantitative numerical analysis was applied to the acquired EIS spectra by fitting to appropriate equivalent circuits. The successful data fitting required pure capacitances (C), instead of Constant Phase Elements (CPE). This fact confirms the purely capacitive properties of the obtained AAO films. The equivalent circuit data fitting has shown that additional CPE was necessary for the data fitting of the spectra, acquired after 336 hours of exposure. This element was ascribed to pore obstruction by $Al_x(OH)_{3x-y}Cl_y$ products. The further data fitting analysis has shown gradual decrease of the capacitances, coupled by simultaneous resistance increment.

On the basis of all data, it was established that the AAO suffer gradual deterioration which decelerates with time. The reason for this deceleration is the access suppression of corrosive species, due to the pore obstruction commented above.

The LSV curves have undoubtedly confirmed the inferences done for the EIS data analysis. All the curves, acquired for the entire period of 5208 hours of exposure were at insignificant currents, approaching the equipment minimum current detection threshold. This fact confirms the statement that the AAO films are able to resist and

do not suffer any breakdowns for the entire exposure period.

Acknowledgements: The authors are grateful for the funding of this research to the Bulgarian National Scientific Research Fund, under contract DFNI-T02-27.

REFERENCES

1. M. Lamberti, F. Escher, *Food Rev. Internat.*, **23**, 407 (2007).
2. O. Ayalon, Y. Avnimelech, M. Shechter, *Envir. Sci. Pol.*, **3**, 135 (2000).
3. C. C. Huang, H. W. Ma, *Sci. Total Env.*, **324**, 161 (2004).
4. K. Marsh, B. Bugusu, *Mater. Envir. Iss.*, **72**, R39 (2007).
5. S. P. Joshi, R. B. Toma, N. Medora, K. O'Connor, *Food Chemistry*, **83**, 383 (2003).
6. M. Šeruga, J. Grgić, M. Mandić, *Z. Lebensm. Unters.Forch.*, **198**, 313 (1994).
7. F. Bianchi, M. Careri, M. Maffini, A. Mangia, C. Mucchino, *Rapid Commun. Mass Spectr.*, **17**, 251 (2003).
8. A. Becaria, A. Campbell, S. C. Bondy, *Toxicol. Ind. Health*, **18**, 309 (2002).
9. J. Kandiah, C. Kies, *Biometals*, **7**, 57 (1994).
10. S. S. Golru, M. M. Attar, B. Ramezanzadeh, *Appl. Surf. Sci.*, **345**, 360 (2015).
11. S. S. Golru, M.M. Attar, B. Ramezanzadeh, *Prog. Org. Coat.*, **87**, 52 (2015).
12. S. S. Golru, M.M. Attar, B. Ramezanzadeh, *J. Ind. Eng. Chem.*, **24**, 233 (2015).
13. D. E. Johnson, T. L. Anderson, US patent, US6559385B1 (2003).
14. C. McCullough, A. Mortensen, P. S. Werner, H. E. Deve, T. L. Anderson, US patent US6180232B1 (1995).
15. X. Y. Huang, P. K. Jiang, *J. Appl. Phys.*, **102**, 124103 (2016).
16. C. Hiel, G. Korzeniowski, D. Bryant, US Patent US7179522B2 (2004).
17. J. Crahay, US Patent, US4322600A (1979).
18. T. M. Smith, US Patent, US3987897A (1975).
19. C. Ralph E., US Patent, US2114072A (1938).

20. J. Curt, US Patent, US2780253A (1950).
21. F. C. Chen, M. K. Chuang, S. C. Chien, J. H. Fang, C. W. Chu, *J. Mater. Chem.*, **21**, 11378 (2011).
22. R. Abdel-Karim, S. M. El-Raghy, Chapter 7 in: Nanofabrication using Nanomaterials, J. Ebothé, W. Ahmed (Eds.) One Central Press (Manchester U.K.) 2016, p. 197 - 218
23. P. Vachkov, D. Ivanov, Gov. Ed. "Tekhnicka" Sofia, 15 (1990).
24. S. Iwauchi, T. Tanaka, *Jpn. J. Appl. Phys.*, **10**, 260 (1971).
25. H. Klauk, *Nature Materials*, **8**, 853 (2009).
26. P. Bocchetta, M. Santamaria, F. Di Quarto, *J. Mater. Sci. Nanotech.*, **1**, 1 (2014).
27. T. Kumeria, A. Santos, D. Losic, *Sensors*, **14**, 11878 (2014).
28. A. Santos, T. Kumeria, D. Losic, *Materials*, **7**, 4297 (2014).
29. H. Kaesche, Corrosion of the Metals, "Metallurgy" Gov. Ed., Moscow, 219 (1984).
30. M. Machkova, E.A. Matter., S. Kozhukharov, V. Kozhukharov, *Corros. Sci.* **69**, 396 (2013).
31. S. Kozhukharov, V. Kozhukharov, M. Wittmar, M. Schem, M. Aslan, H. Caparrotti, M. Veith, *Prog. Org. Coat.*, **71**, 198 (2011).
32. A. A. Salve, S. Kozhukharov, J. E. Pernas, E. Matter, M. Machkova, *J. Univ. Chem. Technol. Metal.*, **47**, 319 (2012).
33. B. A. Boukamp, *Solid State Ionics*, **18/19**, 136 (1986).
34. M. Bethencourt, F. J. Botana, J. J. Calvino, M. Marcos, M. A. Rodriguez-Chacon, *Corros. Sci.*, **40**, 1803 (1998).

КОРОЗИОННА УСТОЙЧИВОСТ НА АНОДНИ ОКСИДНИ СЛОЕВЕ (АОС) ОТЛОЖЕНИ ВЪРХУ ТЕХНИЧЕСКИ ЧИСТА СПЛАВ АА1050

К. А. Гиргинов, С. В. Кожухаров, М. Х. Миланес

Химикотехнологичен и металургичен университет, бул. Климент Охридски №8, 1756 София, България

Постъпила на 03 юни 2017 г.; приета на 07 октомври 2017 г.

(Резюме)

Представени са данни за значителната корозионна устойчивост на анодни оксидни слоеве (АОС), формирани върху техническата алуминиева сплав АА1050. Формирането на оксидните филми е проведено галваностатично (15 mAcm^{-2}) и изотермично ($20 \text{ }^\circ\text{C}$) в 15% H_2SO_4 , в продължениена 48 min. Процесът е провеждан с образци от АА1050 (30x30 mm) в двуелектродна електролизна клетка, при непрекъснато разбъркване на електролита. Изследванията на АОС са проведени след продължително (до 5208 часа) експониране на образците в моделна корозионна среда (3.5% NaCl). Чрез Електрохимична Импедансна Спектроскопия (ЕИС) и Линейна Волтаперометрия (ЛВА) оксидните слоеве са подлагани на регулярни (ежеседмични) електрохимични измервания. Анализът на импедансните спектри показва почти чисто капацитивно поведение на изследваните образци, което се дължи на добре изразената изолаторна способност на оксидните слоеве. Оксидните слоеве запазват своите капацитивни свойства през целия период на експозиция, демонстрирайки много добра корозионна устойчивост. Получените импедансни спектри са подложени на количествен анализ при използване на подходящи еквивалентни схеми. Резултатите получени чрез импедансните спектри за свойствата на АОС са потвърдени и от проведените волтаперометрични измервания. Регистрираните токови плътности (в анодна и катодна посока) потвърждават заключенията за почти чистото капацитивно поведение на формираните АОС. Получените данни показват, че дори след 5208 часово излагане в корозионна среда не се наблюдават забележими корозионни поражения. Това е убедително доказателство, че формираните оксидни слоеве могат ефективно да защитават алуминиевата АА1050 сплав.

Ключови думи: Анодиране, Анодни филми върху алуминий, ЕИС, ЛСВ